Finding Metal-Poor Giants in the Kepler Field for Asterosiesmology

Nathan Harmon, Paul Harding

Case Western Reserve University Department of Astronomy

Abstract

Asterosiesmology is an emerging field that promises the most accurate method of measuring stellar properties yet, but yet has to be properly calibrated for metal-poor stars. We are searching for metal-poor giants in the Kepler field so that precise asteroseismology models of them can be generated, fixing the scaling relations used to derive mass and radius. Candidates are located by comparing their Washington photometry colors. We have located 38 candidates after mapping out nearly a quarter of the Kepler field which will be passed on for asteroseismic modeling.

1. Introduction

Asteroseismology is a new field that promises to be the most accurate method yet for determining the properties of stars, especially so when it comes to their age. Seismic waves propagating within stars cause fluctuations in the luminosity of a star which vary from one part in a hundred in a giant to ten parts in a million for a dwarf[1]. The only telescope capable of measuring these fluctuations on a large scale is the Kepler Space Telescope, which was designed to find planets via the magnitude dip they cause when they pass in front of their star, making it ideally suited for asteroseismology. The frequency of asteroseismic fluctuations depends upon interior properties of the star, such as pressure, temperature, and composition. After careful

observations and detailed models of the sun and other nearby stars, scaling relations for the mass and radius of the star have been developed[2].

$$\frac{M}{M_\odot} \backsimeq \left(\frac{\nu_{max}}{\nu_{max,\odot}}\right)^3 \left(\frac{\Delta\nu}{\Delta\nu_\odot}\right)^{-4} \left(\frac{T_{eff}}{T_{eff,\odot}}\right)^{3/2}$$

$$\frac{R}{R_\odot} \backsimeq \left(\frac{\nu_{max}}{\nu_{max,\odot}}\right) \left(\frac{\Delta\nu}{\Delta\nu_\odot}\right)^{-2} \left(\frac{T_{eff}}{T_{eff,\odot}}\right)^{1/2}$$

The symbol $\odot$ refers to properties of the sun. T_{eff} is the effective temperature, ν_{max} is the frequency of maximum power, and $\Delta\nu$ is the large frequency separation. The temperature is determined by the color of a star or from spectral analysis, and the frequencies can be measured from a Fourier Transform of the star's luminosity observed over a period of months to years.

From mass and radius, most of the other important properties of a star can be calculated, including the age if the metallicity is known[3]. Asteroseismology allows for a direct and more accurate measurement of stellar properties than any other method currently for an individual star. Additionally, asteroseismology is almost unique in that its measurements are obtained without color measurements (See Appendix A for explanation of magnitudes and colors). Because of this, its measurements are independent of the reddening effect caused by interstellar dust.

The issue with these scaling relations is that they are not dependent upon the metallicity of the star (See Appendix B for an explanation of metallicity). A higher metallicity reduces the speed of sound within the star and alters the frequencies. As the sun happens to be a more metal-rich star, the scaling relationships currently only work properly for stars that have similar metallicities and have not been properly tested for stars different from solar composition[4]. We

are finding metal-poor giants so that detailed models can be created of them and studied, allowing for the scaling relations to be extended to metal-poor stars.

We expect metal-poor giants to reside predominately in the galactic halo[5], which formed early in the history of our galaxy and have been kept away from sources of metal pollution. These stars typically have a lower metallicity than the solar neighborhood by two orders of magnitude[5]. Halo stars are rare compared to stars in the disk, but have the advantage of being evenly distributed across the sky, so where we choose to look should not make a difference in how many we find. This does not mean they make up a consistent fraction of the stars we see in a given part of the sky, especially in the Kepler field where we are looking into the upper layers of the galactic disk, increasing the number and density of disk stars we observe. Because of this, metal-poor giant candidates are rare in our fields, roughly one for every 50,000 stars that we observe in an image.

2. Methods

2.1 Observations

Case Western Reserve University's Burrell-Schmidt telescope at Warner-Swasey Observatory in Kitt Peak National Observatory was used for collecting the data. The Schmidt telescope is ideal for the task because it has a large field of view of a degree and a half per side. The Kepler field is quite large at 105 square degrees, so it was necessary to subdivide it into 80 Schmidt sized fields. We use the Washington photometry system, which consists of the C, M, T2, and DDO51 filters, which are highly sensitive to luminosity metal abundances[6] (see Figure 1 for filter response). Each field is imaged four times in each filter, with two long exposures for

dimmer stars and two short exposures for brighter stars. Long exposures are 360 seconds for C and 51 and 60 seconds for i and M, while short exposures are 60 seconds for C and 51, ten seconds for M, and five seconds for i. 32 of the fields were taken and analyzed in previous years. This year, five fields were imaged in May and another 18 in June.

Several images also need to be taken in order to reduce our error and identify outliers. The two additional types of exposures taken to remove instrumental signatures of our equipment are zeros and twilights. Zeros are images taken with zero exposure time, so that the resulting image is just the read out of the CCD. Twilights are taken at twilight, while the sky is still light enough to mask stars. The telescope is pointed at a patch of sky that is flat, meaning that the CCD gets roughly the same number of photons on every pixel. Standard star fields are imaged in every filter to remove the effects of the atmosphere and to provide for a calibration of absolute flux, tying our data into the Washington photometric system. We also image globular clusters of a known metallicity as a self-consistency check.

Figure 1

Washington Filter Response

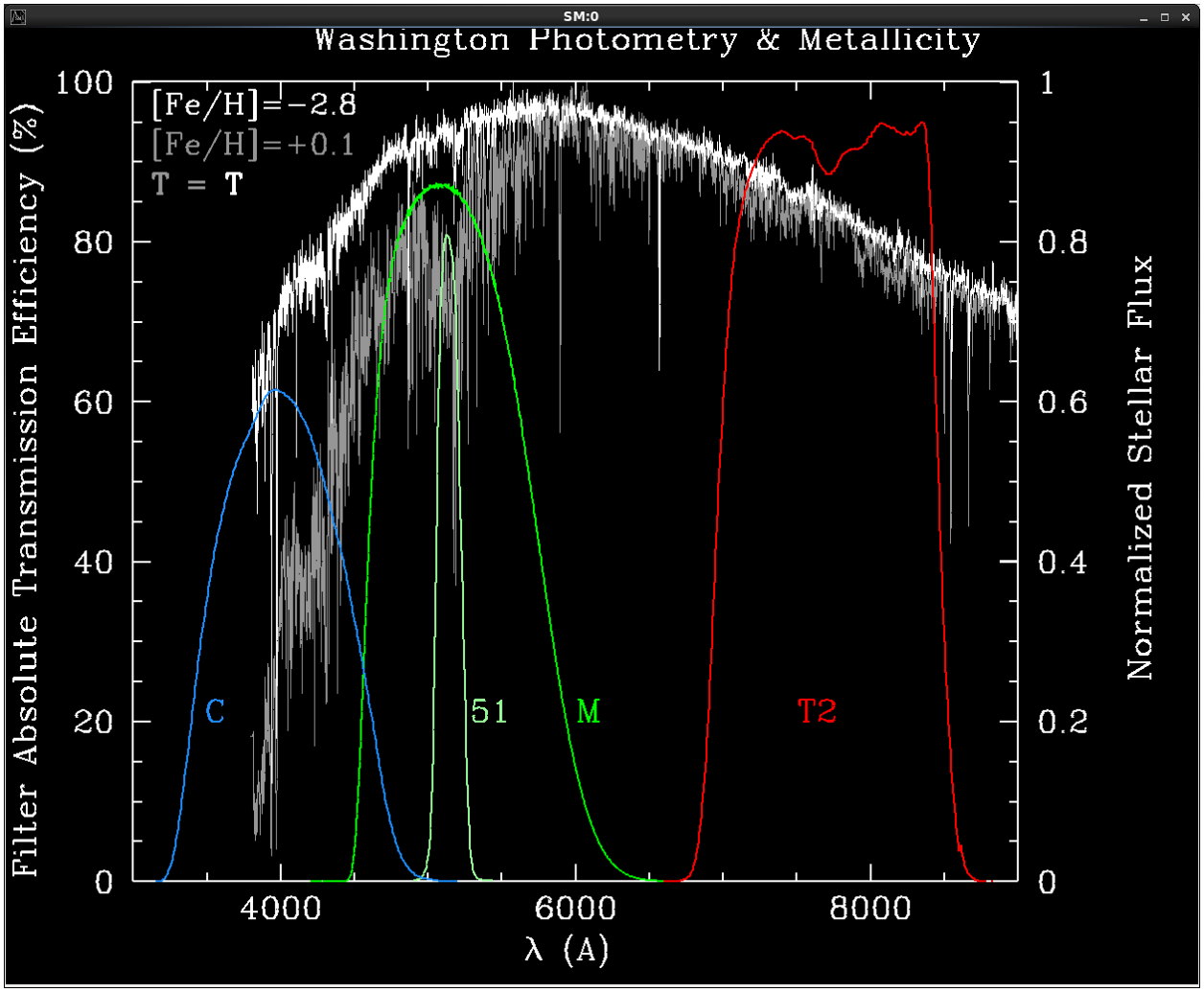

How much light each of the four Washington filters lets in as a function of wavelength. Additionally, two stellar spectra from stars of a similar temperature are shown. Gray is a metal rich dwarf, and white is a metal poor giant. Of special interest is the M-T2 color which acts as a temperature, and the narrow 51 filter centered on a prominent MgH feature. Image courtesy of Thomas Reding.

2.2 Data Reduction

Many sources of noise need to be accounted for in our images. From the zeros we can model thermal noise on the chip and read out noise. Twilights show the bias level introduced by each amplifier, the device that reads out the chip, and lets us correct for the response of the chip. Linearity corrections must also be made to make sure that the image is even across the chip. The goal of all of these corrections is to limit our error to 1%.

The images are cleaned up enough to run through a program called DoPhot[7]. This program calculates a best fit model to all of the flux sources, which is then used to calculate the magnitude of each star in every filter. Each image is checked for magnitude fluctuations from exposure to exposure, which would be indicative of bad seeing conditions and cloud cover. Then corrections for the atmosphere are generated. Standard fields have stars with defined magnitudes for various filters with which we compare our observations against. We generate a linear solution for the disturbances of the atmosphere each run as a function of color and airmass, how much of the atmosphere we are looking through, as well as a sky background zero point for each night.

Once all of the corrections have been made, we compare the metallicity of the globular clusters inferred from our observations against their values in the literature. In each run we imaged the clusters M3, M5, and M92. Our measurements for the clusters were obtained from their position on a M-T2 vs C-M color-color plot (See Table 1 for results). The values from June are close, but the ones from May are significantly off. In addition, the fields in May were showing magnitude variations that are consistent with light cloud cover, and it was judged that they were unusable.

Table 1

Measured metallicities of globular clusters compared to accepted values

Cluster	Literature [Fe/H]	May	June
M3	-1.50	-0.73	--
M5	-1.29	-0.73	-1.26
M92	-2.31	-1.61	-2.37

The Harris[8] [Fe/H] values for three globular clusters compared to our calculated [Fe/H] values for those clusters in both May and June. The June values are fairly close, while the May values are horribly off. There is no June value for M3 due to the computer not finding enough good cluster stars for a reliable calculation.

2.3 Analysis

We match the images to RA and Dec coordinates and compare our measured photometry against the Kepler Input Catalog (KIC), matching our sources to those in the catalog. A computer routine is used to generate a fourth order fit between our data and the KIC, throwing away any source that has a residual greater than 1%. When we are finished calculating the coordinates of the stars, we correct for the reddening from interstellar dust with values from the Schlegel dust maps[9]. The reddening is used for a given field is the average E(B-V) value over the extent of the field, which is then transformed to Washington colors. Our data is then plotted on color-color plots to identify our candidates (See Appendix C for an explanation of the science behind the color-color plots). The M-T2 versus C-M plot is used to pick out stars based on their metallicity (see Figure 2). Isoabundance lines have been calculated for the giants[6]**,** with the [Fe/H] = -1.5 lines falling from ($M\text{-}T2_0$, $C\text{-}M_0$) (1.000, 0.555) to (1.450, 1.199) to (1.800, 1.655). (See explanation in Appendix B for [Fe/H]). However, the isoabundance lines only hold for stars at a similar point in their stellar evolutions, meaning that stars that are not giants can be also

present in the selection area. An M-T2 versus M-DDO51 plot is required to separate out the giants and the dwarfs (see Figure 3). This plot also has the advantage that giants with lower metallicities remain farther out from the dwarfs, allowing us to concentrate on the most metal-poor giants. Points above the box are also selected as giants, as the top is a soft limit. The right and left limits correspond to the edges of the isoabundance lines on the M-T2 versus C-M diagrams, and the left boundary is also where it gets difficult to distinguish between dwarf and giant. We can reasonably expect no metal-poor star to fall below the bottom of the box.

Figure 2

M-T2 versus C-M

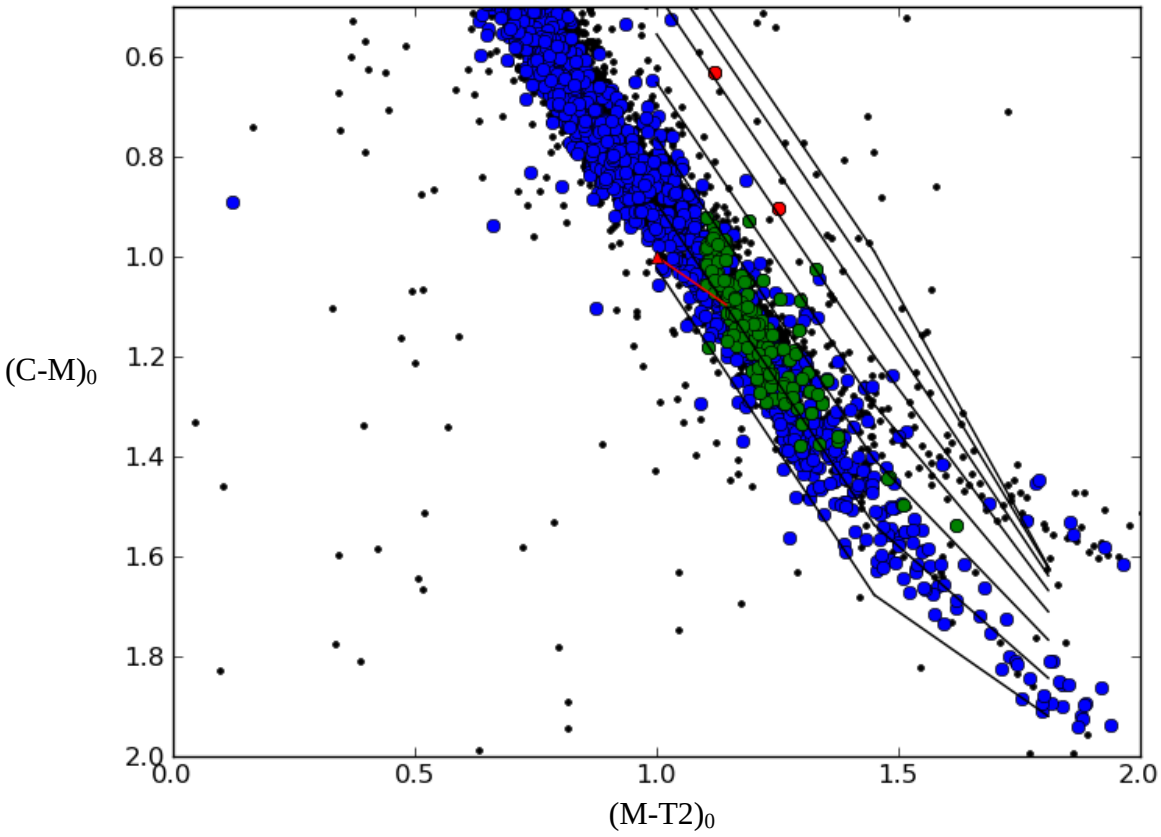

A M-T2 versus C-M diagram from one of our fields. The $_0$ on the color denotes that it has been dereddened. The black points are rejected stars that were either too faint or had errors that were greater than 5%. Blue circles are good stars, green circles are giants determined off an M-T2 versus M-51 diagram, and red circles are metal-poor giant candidates. The red line and triangle shows the reddening vector, how much the data was shifted when it was dereddened. A point at the red triangle would be at the other end of the line before correcting for reddening. The black lines are isoabundance lines, with the second line from the bottom being solar abundance and subsequent lines decreasing by -0.5. Any green circles above the [Fe/H] = -1.5 are colored red and selected as candidates.

Figure 3

M-T2 versus M-51

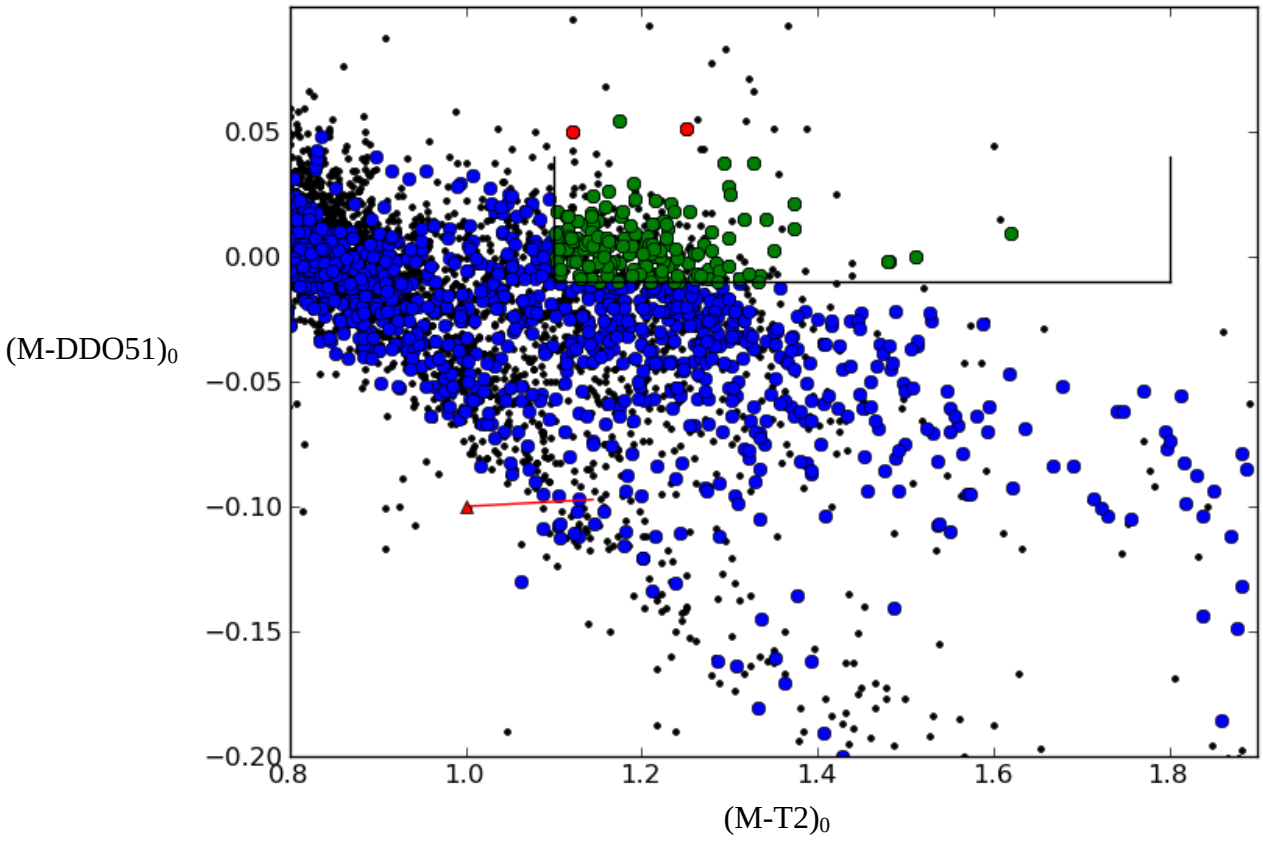

A M-T2 versus M-51 diagram for the same field as Figure 2. The $_0$ on the color denotes that it has been dereddened. The black points are rejected stars that were either too faint or had errors that were greater than 5%. Blue circles are good stars, green circles are giants, and red circles are metal-poor giant candidates as selected off the M-T2 versus M-51 diagram. The red line and triangle shows the reddening vector, how much the data was shifted when it was dereddened. A point at the red triangle would be at the other end of the line before correcting for reddening. In this diagram, dwarfs follow a line along the bottom separating out from the giants, the most metal-poor of which reside along the top. All blue circles that fall in and above the box are selected as giants and colored green.

3. Discussion

It must be noted that our reddening corrections are only estimates. As the dereddening values used are the average value of the entire field, the dereddening for any given star is not precise. This effect is particularly exaggerated in fields that have a larger degree of variation in the amount of dust which are closer to the disk of the galaxy. For the most part, these effects do not affect our data to a large extent, as our candidate selection areas still seem to reside in their proper places and we still observe roughly two candidates per field, as expected. The issue only becomes significant in our two easternmost fields, those closest to the galactic disk. Here it becomes apparent that our dereddening process is significantly overcorrecting, shifting the entire sequence of stars out of our candidate selection regions and almost off the plots entirely. No candidates were selected in these fields. Overcorrections move stars in such a way that fewer candidates are selected, possibly weeding out borderline stars. Overcorrecting is not uncommon, as foreground stars whose light does not have to travel through all of the observed dust will not be affected as much. If our dereddening process overcorrects on all of our fields, then we do not have to worry that there are additional stars being selected as candidates that should not be.

We have identified three possible systematics in locating our candidates. The first scenario which we consider as a possible systematic is whether our flux source is a star or a galaxy. It is possible that our point source is instead a galaxy that is too far away to be resolved or is very concentrated. A red dwarf elliptical would have no or few absorption lines, and could easily float to the top of our giant selection box. However, such a galaxy that is far enough away to be unresolved and bright enough to pass our error cut would be extremely rare, and such objects are unlikely to contaminate our sample.

We also consider systematics from our magnitude calculations. The program DoPhot fits a model to our image, creating a best fit for the observed flux sources[7]. A possible issue arises in crowded fields when dophot is unsure of whether a flux source is a single star or two stars overlapping. If it is divided in some frames and not others, the star will appear much brighter in the frames where it was not split, and could potentially move the source into our candidate selection region. A simple visual check of each of our candidate is sufficient to see if this is the case.

Finally, we also consider the case should a star fall upon or near a bad pixel on our CCD. Such an instance will make the star appear much dimmer in that frame, and could have the same effect as the case stated above. Once again, a simple visual check will reveal if this is an issue.

4. Conclusions

After analyzing our 18 fields, we find a total of 38 candidates. 15 of these candidates appear in both the long and short exposures, the repeated observations making them our most likely candidates. Additionally another 15 appeared only in the short exposures, being bright enough to saturate the CCD in the longer exposures, and another 8 only in the long exposures, being too dim to gather enough light for meaningful results in the short exposure. The RA Dec coordinates of our candidates are listed in Table 2.

These candidates will be passed on to Courtney Epstein at Ohio State University, who is working on extending the asteroseismology scaling relations to the metal-poor regime. Her work with some of our previous candidates indicates that the masses derived for metal-poor stars with

the scaling relationships is 16% too high[4]**.** Our additional candidates will allow her to better constrain her data, and we will continue to map out the Kepler field, finding new candidates.

Table 2

RA and Dec coordinates of our candidates

Both Exposures	**Short Exposures Only**	**Long Exposures Only**
292.5526, 47.73634	292.8213, 50.06649	292.311, 48.58776
292.3416, 50.72469	292.806, 51.79132	292.6964, 50.54122
292.5899, 50.0561	292.7402, 45.80131	293.2565, 39.10082
292.5272, 44.9395	292.738, 45.54692	293.5145, 37.61317
292.4052, 39.75752	293.6113, 39.09103	282.9409, 47.29478
291.7546, 37.3302	291.9828, 37.30472	281.355, 43.34295
292.3098, 48.58715	293.3634, 36.81548	278.8595, 44.0329
297.8034 ,49.05038	293.5767, 36.57954	280.0471, 43.32097
299.4901, 48.06334	292.0998, 36.21431	
282.5268, 44.40034	295.5928, 37.6953	
282.6703, 43.75409	282.6902, 47.35411	
282.7177, 43.66922	282.1851, 45.7285	
279.7521, 44.58359	281.7297, 45.01468	
278.9472, 44.25159	282.2623, 40.60004	
280.5411, 43.95133	279.4586, 44.45259	

The Right Ascension and Declination of our candidates that appeared in both long and short exposures, or only long or only short exposures.

Aknowledgements

I would like to thank Thomas Reding for his help in collecting the data.

References

[1] Gillilan, R., & Brown, T. 1992, ASP, 104, 677

[2] Kjeldsen, H., & Bedding, T. R. 1995, A&A, 293, 87

[3] Ulrich, R. K. 1986, ApJ, 306, L37

[4] Epstein, C., et al. 2014, ApJ, 785, L28

[5] Rodrigo A. Ibata *et al.* 2014 ApJ, 780, 128

[6] Geisler, D., Claria, J., and Minniti, D. 1991, AJ, 102, 1836

[7] Schecter, P., Mateo, M., and Saha, A. 1993, ASP, 105, 693

[8] Harris, M. 2010, http://physwww.physics.mcmaster.ca/~harris/mwgc.dat

[9] Schlegel, D., Finkbeiner, D., and Davis, M. 1998, ApJ, 500, 525

Appendix A

Magnitudes and Colors

The magnitude system is how astronomers quantify how luminous an object is. The magnitude system is a log base ten scale, with a difference of five magnitudes corresponding to a factor of a hundred in luminosity. Due to historical conventions, the magnitude system is actually backwards, so that more negative magnitudes are brighter. The full moon has a magnitude around -12.7, while you can just barely see magnitude 5 stars with the naked eye. Vega is defined as the zero point in all filters, which for the V-band (centered at 5450 Å) corresponds to a flux of 3.63×10^{-9} erg s^{-1} cm^{-2} $Å^{-1}$.

Colors are the comparison of two filters. The B-V color is the magnitude of the V filter subtracted from the magnitude of the B filter. By convention, the bluer filter (the filter centered on the shorter wavelength) is listed first, so that smaller numbers correspond to bluer, and higher numbers correspond to redder. As Vega is the zero point in all filters, a negative color means bluer than Vega, but as Vega is a fairly blue star, positive numbers can still correspond to blue. As the color is the comparison of two filters, the flux of the object is irrelevant, so color measurements are independent of luminosity and distance from the star.

Appendix B

Metallicity

The metallicity is the metal content of a star. 99% of the mass in the universe is made up of either Hydrogen or Helium, so astronomers call everything that makes up the remaining 1% a metal. Metallicity is most commonly quoted in terms of [Fe/H], where [Fe/H] is defined as

$$\left[\frac{Fe}{H}\right] = \log\left(\frac{\frac{Fe}{H}}{\frac{Fe_{\odot}}{H_{\odot}}}\right)$$

Here the symbol ⊙ denotes the sun, so the metallicity is the log of the ratio of a star's iron to hydrogen ratio compared to that of the sun's. From this is follows that [Fe/H] = 0 is solar composition, [Fe/H] = 1 is a star with 10 times more iron atoms per hydrogen atoms than the sun, and a metallicity of [Fe/H] = -2 has 100 times fewer iron atoms per hydrogen atom than the sun does.

Appendix C

Color-color diagrams

The M-T2 versus C-M diagram is used to differentiate between the metallicities of stars. The M-T2 color is a proxy for temperature, as these two filters are near the peak of the star's

Plank functions. Most of the absorption lines appear in the C filter, so for a given temperature, we expect a variation in the C-M color which corresponds to the metallicity. As a result of this, isoabundance lines are generated in the plot, lines upon which all points have the same metallicity. It is worth pointing out that the spread of the isoabundance lines are why the Washington photometry system was chosen. All filter sets are capable of generating these isoabundance lines, but the Washington system has the largest separation between isoabundance lines, meaning that it can measure metallicities with the greatest precision.

The problem with the isoabundance lines is that they only work for stars that are in a similar stage of their lives. This means that dwarfs and giants have different sets of isoabundance lines, so that if we try to pick out metal-poor giants, we could also be including dwarfs. The solution for this is to pick out the giants from the dwarfs using a second color-color diagram, M-T2 versus M-DDO51. Once again, the M-T2 color is acting as a proxy for temperature. The M and DDO51 filters are centered on very close to the same color, the difference being that the DDO51 filter is very narrow and centered on some magnesium features. Dwarfs, being smaller stars, have a higher surface gravity which accents the MgH broad line, lowering the DDO51 magnitude, but not so much the M magnitude. Additionally, there is a sharp magnesium atomic line that appears in metal-rich stars. Therefore, the stars that we are interested in on the M-T2 versus M-DDO51 diagram are those with the largest DDO51 to M ratio.